Measurement of Guide Wavelength in Rectangular Dielectric Waveguide

HAROLD JACOBS, FELLOW, IEEE, GABRIEL NOVICK, MEMBER, IEEE, CHARLES M. LoCASCIO, AND METRO M. CHREPTA

Abstract—**Oscillators in the microwave and millimeter-wave region were constructed wherein the resonators consisted of sections of rectangular dielectric waveguide. While adding thin blocks of dielectric to increase the mechanical length of the resonator, the power output and frequency were measured. Using this technique, the experimental value of the wavelength in the longitudinal direction, λ_g, was determined. These experimental data were then compared with calculations predicted by optical theory. Good agreement was found where the bulk wavelength was small compared with the cross-sectional dimensions of the dielectric. If the half-wavelength in the dielectric was comparable with the dielectric dimensions, the values of λ_g were greater than the theoretical values.**

In the process of carrying out these experiments, a new type of oscillator is described which provides a power output comparable with diodes in metal-walled cavities. In addition, the new dielectric cavities are simple in construction and are compatible with dielectric waveguide, image line, or microstrip systems.

I. Introduction

IN THE RECENT LITERATURE, several articles [1]–[5] have appeared describing propagation of electromagnetic radiation in dielectric waveguide, image line, dielectric strip line, and other configurations in which dielectrics are used for guiding the energy rather than metal-wall structures. The reason for this interest is that in the regions of wavelength from 5 mm to optical wavelengths the metal-wall structures cause attenuation due to skin effect losses. These skin effect losses, denoted by the attenuation constant α_c, are proportional to the square root of the frequency. In the case of dielectric losses (denoted by α_d), these losses are due to the shunt conductance of the dielectric, and depend on the resistivity or polarization and the dimensions of the dielectric material. In general, the dielectric losses α_d can be made much less than the conduction losses α_c at high frequencies. In the millimeter-wave region, for high-resistivity silicon or Al_2O_3 dielectric lines, α_c is often more than ten times the value of α_d, when comparing metal waveguide to dielectric waveguide propagation. In the experiments described in this paper, a Gunn diode was imbedded in a rectangular dielectric cavity. This was done to examine the feasibility of using dielectrics with minimal metal structures as resonant cavities for oscillators. The reasons for examining dielectric cavities as resonators are twofold. First, if proven feasible, this might be a more compatible technology for use with dielectric line and/or microstrip circuitry. Second, this technology might prove less costly than metal-walled structures which require precision machining inside the structural assembly.

Manuscript received November 11, 1975; revised May 12, 1976.

H. Jacobs and M. M. Chrepta are with the U.S. Army Electronics Command, Electronics Technology and Devices Laboratory, Fort Monmouth, NJ 07703.

G. Novick and C. LoCascio are with Monmouth College, West Long Branch, NJ.

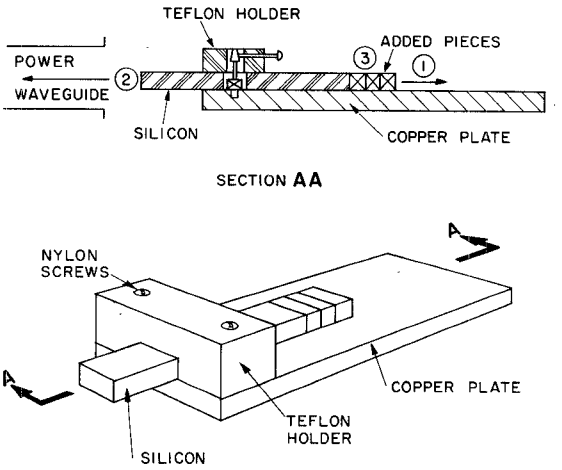

Fig. 1. Dielectric cavity structure, 38.6 mm long.

In the process of evaluating the performance of high-resistivity dielectric resonators, measurements were also made on the guide wavelength λ_g by adding small blocks of dielectric material to change the longitudinal dimensions of the cavity. The determination of λ_g will be of great importance in checking the accuracy of various theories proposed concerning the propagation characteristics of these lines. The experiments to be described were largely carried out in the region of 10–15 GHz for quantitative data. Later, for specific questions concerning scaling, demonstrations were carried out at 60 GHz.

II. Experimental Methods

The dielectric cavity design was constructed as follows. In the first arrangement, shown in Fig. 1, the silicon was machined and polished with a rectangular cross section 3.5 mm high and 7.0 mm wide. The length was 38.6 mm and additional pieces could be added to change the line length of the dielectric resonator. A hole was cut, 3 mm in diameter, in the center of the basic silicon resonator and an *X*-band Gunn diode was inserted. A Teflon holder was used to clamp the silicon down onto a copper plate while at the same time serving as a holder for the top terminal of the diode. A fine wire or very thin screw was placed in the longitudinal direction to make contact to the positive terminal of the diode.

The silicon resistivity was of the order of 10000 $\Omega \cdot$ cm as were the pieces to be added for tuning purposes. Two

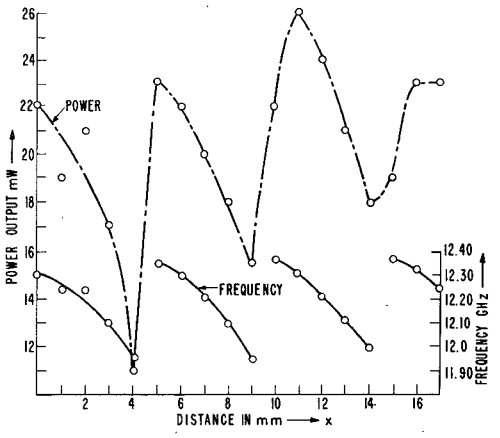

Fig. 2. Power and frequency as a function of added resonator length, with no tuning disk added: $\lambda_g = 10.0$ mm.

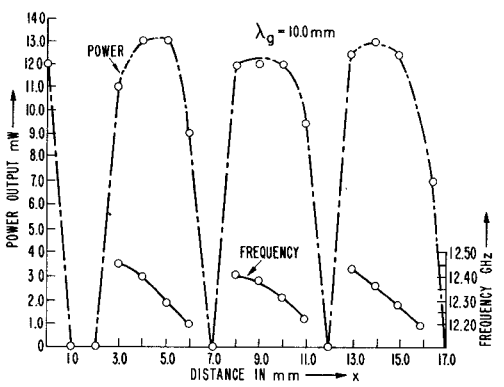

Fig. 3. Power and frequency as a function of added resonator length, with a 7-mm tuning disk added: $\lambda_g = 10.0$ mm.

nylon screws were used to clamp the Teflon holder to the copper plate and were located near the outer edges on either side of the silicon. A waveguide was used to couple the power out of the silicon cavity. Behind this a standard waveguide arrangement was used to measure power and frequency, and to monitor the spectral output by means of a spectrum analyzer.

Using the 38.6-mm-long silicon resonator, the front edge of the silicon was approximately 5 mm away from the waveguide used for the measurements. As added pieces were placed on the line, both power and frequency were monitored. The results are shown in Fig. 2. The data showed that as the line length is increased there is a periodicity in frequency as well as output power. The guide wavelength, determined experimentally, is about 10 mm. In a computer analysis, using Marcatili's formulation, $\lambda_g = 9.0$ mm, for the cross-sectional dimensions used.

Next, the same arrangement was used as in Fig. 1, except a metallic disk was connected to the top terminal lead of the diode. The metal disk was located between the silicon upper surface and the Teflon holder. Different disks were tried with varying diameters. The optimum disk diameter was found to be 7 mm and the thickness, although not critical, was less than 0.5 mm. The data are shown in Fig. 3; the power and frequency are given as a function of added line length, and, again, we see that for a frequency of 12.3 GHz λ_g is about 10 mm.

In the next series of experiments, dielectric resonators were used with shorter lengths. Here, the dimensions of the silicon piece were: 3.5 mm high, 7.0 mm wide, and 18.0 mm long. Again, in the center of the silicon is a hole, 3 mm in diameter, into which the Gunn diode can be inserted. The diode and silicon were clamped down with a Teflon strap, and the center conductor of a thin coaxial wire was used to provide positive bias to the top terminal of the diode—the outer conductor being connected to ground. The shorter resonator completely prevented multimoding which had been observed on some occasions in some of the longer pieces. With the shorter resonator, runs were made measuring power and frequency as a function of line length

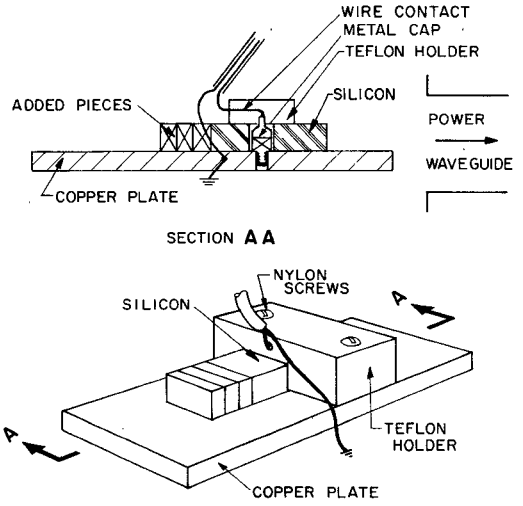

Fig. 4. Dielectric cavity structure, 18.0 mm long.

added to the rear portion of the dielectric resonator. In addition, the copper image plane was made large enough so that the front and rear portions of the silicon rested on the ground plane and the copper plate extended in front of the silicon by about 10 mm. This copper plate extended 12 cm in the backward direction as shown in Fig. 4. The data for the case of no tuning disks present are shown in Fig. 5. With a 6-mm-diam metallic disk added on top of the silicon, power output was increased (doubled); the data are given in Fig. 6. These data were taken with the end of the semiconductor 3.5 mm away from the waveguide used for measurement. The distance was chosen for optimum coupling into the waveguide with no added pieces attached.

III. Discussion of Wavelength

The repetition of the power output and frequency when plotted as a function of the added dielectric length is shown in Figs. 2, 3, 5, and 6. This repetition of the power output and frequency occurs once every half-wavelength. The actual frequency variation can be calculated by making the transmission line analysis of the dielectric waveguide cavity, as shown in Appendix A, and neglecting the losses. Curves C and D of Fig. 11 correspond to the frequency variation

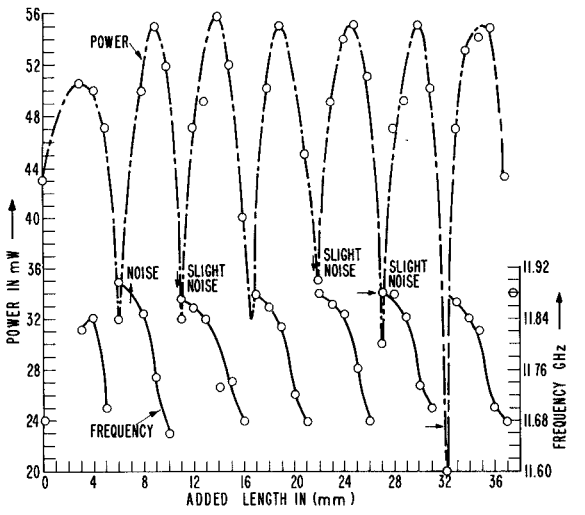

Fig. 5. Power and frequency as a function of added resonator length, with no tuning disk added, for a shorter cavity: $\lambda_g = 10.6$ mm.

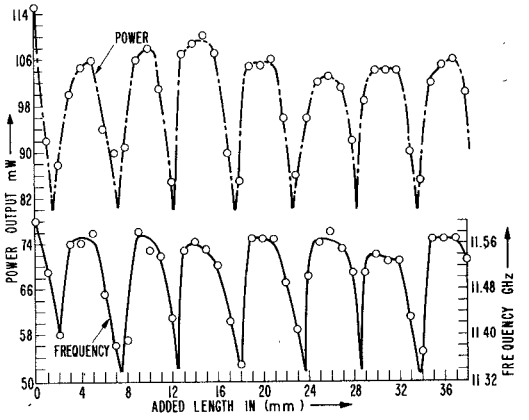

Fig. 6. Power and frequency as a function of added resonator length, with a 6-mm tuning disk added, for a shorter cavity: $\lambda_g = 10.7$ mm.

in Fig. 2; curves A and B of Fig. 10, with the heavier capacitive loading of the diode, correspond to the smaller frequency variation in Fig. 3.

The data in Figs. 2, 3, 5, and 6 illustrate a direct measurement of λ_g, the wavelength in the longitudinal direction. Theoretically, the guide wavelength in the dielectric is dependent upon what fraction of the propagating wave is outside the dielectric as an evanescent part and what fraction of the wave is inside the dielectric. In general, the larger the fraction in air, the longer the wavelength and conversely, the larger the fraction in the dielectric, the shorter the wavelength. As the frequency increases further, the guide wavelength of the electromagnetic radiation approaches the wavelength in the bulk dielectric. This reasoning is based on the theory presented by Marcatili. Using the experimental technique described above and choosing different Gunn diodes, we were able to change the frequency of oscillation. Then, by adding lengths to the dielectric resonator, we could determine λ_g experimentally for various frequencies with the same cross-sectional silicon pieces. It was found that for a diode with oscillations at

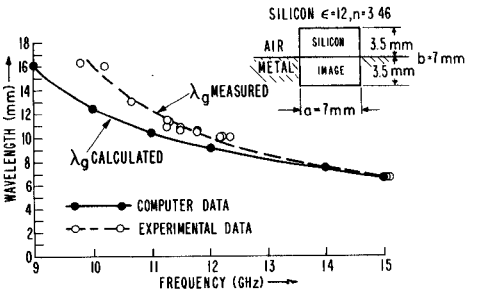

Fig. 7. Calculated and measured guide wavelength λ_g as a function of frequency.

10.2 GHz the wavelength was 16 mm. For a diode oscillating at about 12.0 GHz, λ_g was 10 mm, and for diodes operating at about 15.0 GHz, λ_g was about 6.8 mm.

Next, consider a quantitative description of how the above processes work. We will start by using the theoretical formulation developed by Marcatili and compare this with the data. This is of interest since in his paper Marcatili [1] pointed out that his equations would become less accurate as the dimensions of the dielectric waveguide were made comparable with the half-wavelength in the infinite medium. In Fig. 7, the results of calculations of the guide wavelength, in a silicon transmission line with the dimensions indicated are plotted. Here λ_g has been calculated with the help of the computer using the following equations as derived by Marcatili:

$$k_x a = \pi - \tan^{-1}(k_x \xi_3) - \tan^{-1}(k_x \xi_5) \tag{1}$$

$$k_y b = \pi - \tan^{-1}\left(\frac{n_2^2}{n_1^2} k_y \eta_2\right) - \tan^{-1}\left(\frac{n_4^2}{n_1^2} k_y \eta_4\right) \tag{2}$$

$$\xi_{3,5} = \frac{1}{\left(\left[\frac{\pi}{A_{3,5}}\right]^2 - k_x^2\right)^{1/2}} \tag{3}$$

$$\eta_{2,4} = \frac{1}{\left(\left[\frac{\pi}{A_{2,4}}\right]^2 - k_y^2\right)^{1/2}} \tag{4}$$

$$A_{2,3,4,5} = \frac{\lambda_0}{2(n_1^2 - n_{2,3,4,5}^2)^{1/2}} \tag{5}$$

where λ_0 is the free space wavelength; n_1 is the index of refraction of the silicon dielectric; $n_2, n_3, n_4, n_5 = 1$ for air; $\xi_{3,5}$ are the field attenuation constants in the x direction; $\eta_{2,4}$ are the field attenuation constants in the y direction; and

$$k_z^2 = k_1^2 - k_x^2 - k_y^2$$

$$k_z = \frac{2\pi}{\lambda_g}. \tag{6}$$

The cross-sectional dimensions used in these calculations of the dielectric waveguide were 7.0 mm × 7.0 mm. This was done since the actual experiment utilized an image line configuration with the silicon 3.5 mm in height and 7.0 mm

in width. Both arrangements can be shown to be equivalent [6]. In addition, the calculations based on (1)–(6) were carried out with the computer utilizing the values of the transcendental equations and not requiring small values of the arguments k_x, ξ_3 as has been done using approximation techniques.

We can now compare the measured values of λ_g with the computer calculations which utilized (1)–(6). Fig. 7 shows the measured values of λ_g as well as the calculated values of λ_g. This illustrates that as the wavelength becomes smaller with respect to the cross-sectional dimensions of the guide, greater accuracy is found in the calculations.

With this background, the effective index of refraction and, hence, the wave impedance can be obtained. It is noted that the dielectric constant of the infinite medium of silicon is about 12.0, the index of refraction being 3.46. The following definition of n_{eff} was used:

$$n_{\text{eff}} = \frac{\lambda_0}{\lambda_g} \tag{7}$$

where n_{eff} = effective index of refraction, λ_0 = free space wavelength, and λ_g = experimental guide wavelength.

With this definition, and using experimental values of λ_g, we have

$$n_{\text{eff}} = \frac{3.0}{1.6} = 1.88, \qquad \text{at 10.2 GHz}$$

$$n_{\text{eff}} = \frac{2.5}{1.0} = 2.5, \qquad \text{at 12.1 GHz}$$

$$n_{\text{eff}} = \frac{2.00}{0.68} = 3.0, \qquad \text{at 15.1 GHz.}$$

The wave impedance can be calculated at various frequencies. Given

$$Z = \sqrt{\frac{\mu_0}{\varepsilon_0}} \frac{1}{n_{\text{eff}}} \tag{8}$$

where Z = the wave impedance of the line, $(\mu_0/\varepsilon_0)^{1/2}$ = the wave impedance of free space, and n_{eff} is the effective index of refraction of the medium, we obtain the following results: at 10.2 GHz, $Z = 376/1.88 = 200\ \Omega$; at 12.1 GHz, $Z = 376/2.5 = 150\ \Omega$; and at 15.1 GHz, $Z = 376/3 = 128\ \Omega$. As the frequency increases the wave impedance approaches that value found in the infinite bulk material, $Z = 376/3.46 = 108$.

IV. Radiation Patterns

The question may arise as to what the radiation patterns consist of for the dielectric resonant oscillator. To determine this, the entire structure shown in Fig. 4 was rotated in azimuth and elevation angles, using the open metal waveguide structure nearby to sense the radiative power and frequency. In these rotations the diode was used as the pivotal point and was maintained at a distance of approximately 5 cm from the end of the metal waveguide system.

The power intercepted by the waveguide versus azimuthal angle is shown in Fig. 8, and the power intercepted by the waveguide versus elevation is shown in Fig. 9. The half-power points in the plane are symmetric and show a beam angle of about 28°. The elevation angles are tilted upward due to the presence of the copper metal image plane under the silicon image line. It is interesting that the radiation to the side is zero and the perpendicular radiation upward is zero. Most of the power radiated is in the forward (and backward) direction. One explanation [7] for this radiation pattern is as follows: Suppose the dielectric is an even multiple of wavelengths long and is in a resonant state, then the standing electromagnetic waves can be looked upon as effective dipoles. Looking from the front, we see dipoles moving up and down coherently. Looking from the side, we see the same dipoles, but they are in alternate polarities so that cancellation of the radiation occurs and the net resultant radiation is zero. An alternate explanation is as follows: Electromagnetic waves travel in the $+z$ and $-z$ directions. Note that inside the dielectric the constant phase fronts are perpendicular to the z direction [8]. Outside the dielectric, the constant phase fronts are inclined toward the z direction such that the evanescent wave outside the dielectric has a component of velocity going into the dielectric. This is why the dielectric guides the electromagnetic wave and there is no radiation from the sides, top, or bottom. The cavity can be looked upon as a folded dielectric waveguide. The diode generator has been found experimentally not to scatter the radiation. It merely reinforces the radiation in phase with the propagation. This concept of a reinforced traveling wave has been used in laser theory where the molecule in an inverted state releases its energy in phase with the propagating wave.

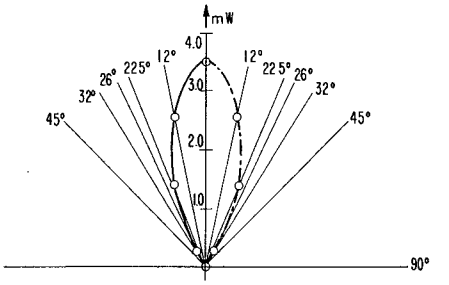

Fig. 8. Power intercepted by the waveguide versus azimuthal angle from the long axis of the silicon resonator.

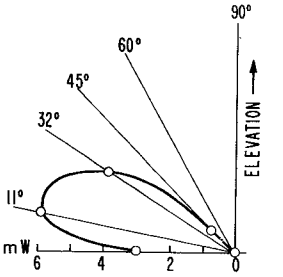

Fig. 9. Power intercepted by the waveguide versus elevation angle measured from the axis of the silicon resonator.

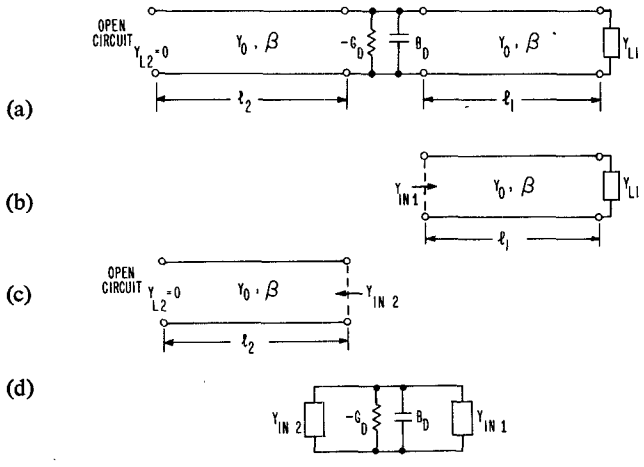

Fig. 10. Equivalent circuit diagrams of the dielectric cavity oscillator.

V. Conclusion

A dielectric oscillating cavity has been suggested using a small amount of metal. The power output is comparable with metal-walled cavity oscillators. By extending the length of the cavity, an experimental method has been set up to measure the guide wavelength λ_g. These data are compared with Marcatili's theory, and it is shown that, for given guide dimensions, the experimental wavelengths are longer than that predicted by theory at longer wavelengths or lower frequencies. The radiation patterns indicate that most of the power is radiated by waves in the longitudinal direction.

This dielectric resonator raises the possibility of a new technological approach to microwave and millimeter-wave active devices with a considerable simplification in construction and cost.

Appendix A
Dielectric Waveguide Cavities: Transmission Line Analysis

It is a known fact that a section of any type of wave-guiding structure can be used as a cavity. The literature [10] has shown that any type of wave-guiding structure can be represented as a transmission line, if the proper values of the propagation constant β and the characteristic admittance Y_0 are used. Here, a theoretical approach will be presented to explain the above experimental results.

Suppose that our dielectric cavity can be represented as a transmission line with a characteristic admittance Y_0 and propagation constant β. Then our dielectric cavity can be represented by Fig. 10(a). In the center of the figure, $-G_D$ and B_D represent the negative conductance and the positive susceptance due to the diode, respectively. Y_0 and β represent the characteristic admittance and propagation constant of our transmission line, where one section of our transmission line has length l_1 and is terminated in load admittance Y_{L1}, and the other section of the transmission has length l_2, and is terminated in an open circuit ($Y_{L2} = 0$). Our dielectric has a resistivity of approximately 10 000 $\Omega \cdot$ cm; hence, for all practical purposes, the attenuation of the transmission line is negligible. Therefore, the lossless transmission line equations shall be used, relating the relative admittance at one point to that at another point. They are as follows:

$$y_{in} = \frac{y_L + j \tan \beta l}{1 + j y_L \tan \beta l} \tag{A-1}$$

$$y_{in} = \frac{Y_{in}}{Y_0} \tag{A-2a}$$

$$y_L = \frac{Y_L}{Y_0}. \tag{A-2b}$$

With the aid of (A-1) and (A-2), the load admittances will transform through the transmission lines, as shown in Fig. 10(b) and (c), into the input admittances, given below:

$$Y_{in_1} = Y_0 \frac{(Y_{L1}/Y_0) + j \tan \beta l_1}{1 + j(Y_{L1}/Y_0) \tan \beta l_1} \tag{A-3}$$

$$Y_{in_2} = j Y_0 \tan \beta l_2. \tag{A-4}$$

From (A-3) and (A-4), the equivalent lumped element circuit diagram of the dielectric cavity is obtained, as shown in Fig. 10(d). By means of Kirchhoff's law, the total admittance of the equivalent lumped element circuit must be equal to zero for a constant amplitude sinusoidal oscillation to exist, namely,

$$Y_{in_1} + Y_{in_2} - G_D + jB_D = 0. \tag{A-5}$$

Equation (A-5) is an equation of complex numbers and, therefore, can be rewritten into two equations of real numbers; namely,

$$\text{Im}\,(Y_{in_1}) + Y_0 \tan \beta l_2 + B_D = 0 \tag{A-6}$$

$$\text{Re}\,(Y_{in_1}) - G_D = 0. \tag{A-7}$$

Equation (A-6) determines the frequency of the oscillation, while (A-7) determines the power output and whether or not the oscillation can be sustained. In order to calculate l_2 as a function of frequency, a normalized form of (A-6) and (A-3) shall be used; namely,

$$\text{Im}\,(y_{in_1}) + \tan \beta l_2 + b_D = 0 \tag{A-8}$$

where

$$y_{in_1} = \frac{y_{L1} + j \tan \beta l_1}{1 + j y_{L1} \tan \beta l_1} \tag{A-9}$$

and it is assumed that

$$b_D = \frac{B_D}{Y_0} = \frac{\omega C_D}{Y_0}. \tag{A-10}$$

Since y_{L1}, in (A-9), is equal to a very small number,

$$y_{L1} \ll 1$$

the right-hand term of the denominator in (A-9) is negligible compared to one and

$$y_{in_1} \approx y_{L1} + j \tan \beta l_1. \tag{A-11}$$

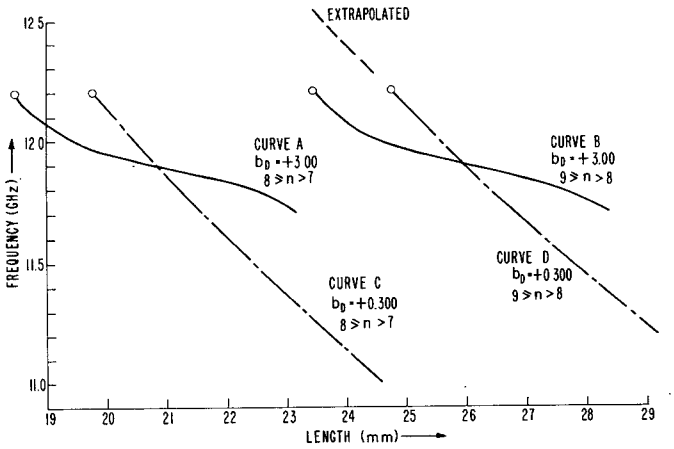

Fig. 11. Calculated resonant frequency as a function of l_2 which represents the distance from the diode to the end of cavity. Curves A,B: Frequency vs length for distances one-half guide wavelength apart, $b_D = 3.00$. Curves C,D: Frequency vs length for distances one-half guide wavelength apart, $b_D = 0.300$.

Thus (A-8) can be written as

$$\tan \beta l_1 + \tan \beta l_2 + b_D = 0 \qquad \text{(A-12)}$$

with the reservation that the value of βl_1 be calculated, to determine whether it is equal to 90° or close thereto, and recorded.

In order to simplify the calculations, the value of b_D, as given in (A-10), shall be considered a constant since the frequency variation is small, namely, $b_D = +3.00$ for curves A and B and $b_D = +0.300$ for curves C and D in Fig. 11. In addition, the assumption will be made that the product of the guide wavelength and the frequency is a constant; this essentially assumes that β is directly proportional to frequency.

The points calculated are plotted in Fig. 11. Note that in Fig. 11 curve D has been extrapolated to lower values of l_2 or higher frequencies. So for $l_2 = 24$ mm and $b_D = +0.300$, two frequencies are possible, namely, 11.14 GHz (from curve C) and 12.40 GHz (from the extrapolated portion of curve D). Note that it is the diode and its negative conductance which show a preference for the lower frequency and prevent operation on the extrapolated portion of curve D.

Acknowledgment

Acknowledgment should be made to K. L. Klohn and J. F. Armata for their computer calculations on the propagation characteristics of radiation in silicon [9].

References

[1] E. A. J. Marcatili, "Dielectric rectangular waveguide and directional coupler for integrated optics," *Bell Syst. Tech. J.*, vol. 48, pp. 2071–2102, Sept. 1969.
[2] R. M. Knox and P. P. Toulios, "Integrated circuits for the millimeter through optical frequency range," in *Proc. Symp. Submillimeter-waves*. Brooklyn, NY: Polytechnic Press, Polytechnic Institute, 1970.
[3] H. Jacobs and M. M. Chrepta, "Electronic phase shifter for millimeter-wave semiconductor dielectric integrated circuits," *IEEE Trans. Microwave Theory Tech.*, vol. MTT-22, pp. 411–417, April 1974.
[4] J. C. Wiltse, "Some characteristics of dielectric image lines at millimeter wavelengths," *IRE Trans. Microwave Theory Tech.*, vol. MTT-7, pp. 65–70, Jan. 1959. Also see D. D. King and S. P. Schlesinger, "Losses in dielectric image lines," *IRE Trans. Microwave Theory Tech.*, vol. MTT-5, pp. 31–35, Jan. 1957.
[5] Y. Chang and H. J. Kuno, "Millimeter wave integrated circuits," Contract DAAB07-74-C-0454, Final Rep., Sept. 1974.
[6] E. C. Jordan and K. G. Balmain, *Electromagnetic Waves and Radiating Systems*. Englewood Cliffs, NJ: Prentice Hall, 1968, pp. 273–275.
[7] Dr. Felix Schwering, private communication.
[8] H. Kogelnik, "An introduction to integrated optics," *IEEE Trans. Microwave Theory Tech.*, vol. MTT-23, pp. 2–16, Jan. 1975.
[9] K. Klohn and J. Armata-T.R., "Transverse propagation constants in dielectric waveguides," U.S. Army Electronics Command, Fort Monmouth, NJ, Tech. Rep. 4242, August 1974.
[10] N. Marcovitz, *Waveguide Handbook*, vol. 10, (M.I.T. Series). New York: McGraw-Hill, 1951.